Front. Struct. Civ. Eng. 2018, 12(3): 425–437
https://doi.org/10.1007/s11709-017-0427-5

RESEARCH ARTICLE

Proposal of a probabilistic assessment of structural collapse concomitantly subject to earthquake and gas explosion

Gholamreza ABDOLLAHZADEH*, Hadi FAGHIHMALEKI

Department of Civil Engineering, Babol Noshirvani University of Technology, Shariati Av., Babol, Mazandaran, Iran
**Corresponding author. E-mail: abdollahzadeh@nit.ac.ir*

ABSTRACT In recent decades, many public buildings, located in seismic-prone residential areas, had to grapple with abnormal loads against which the structures were unguarded. In this piece of research, an ordinary three dimensional reinforced concrete building is selected as case study. The building is located in an earthquake-prone region; however, it is designed according to seismic building codes. Yet, it is not shielded against abnormal loads, such as blasts. It is assumed that the building suffers a blast load, due to mechanical/thermal installation failure during or after intense seismic oscillations. These two critical incidents are regarded codependent and compatible. So the researchers developed scenarios and tried to assess different probabilities for each scenario and carried out an analysis to ensure if progressive collapse had set in or not. In the first step, two analysis models were used for each scenario; a non-linear dynamic time history analysis and a blast local dynamic analysis. In the second step, having the structural destructions of the first step in view, a pushdown analysis was carried out to determine the severity of progressive collapse and assess building robustness. Finally, the annual probability of structural collapse under simultaneous earthquake and blast loads was estimated and offered.

KEYWORDS gas blast, pushdown analysis, progressive collapse, annual probability of structural collapse, 3D model of structure

1 Introduction

Recently Rong and Li [1] undertook a probabilistic assessment of the effect of potential blast loadings and their resultant damage scale on building structures. Using Monte-Carlo simulation and single-degree-of-freedom (SDOF) system, they examined the maximum displacement and displacement ductility factor of a reinforced concrete structure with flexural frames under blast loadings. Stewart and Netherton [2] developed a probabilistic risk assessment (PRA) procedure to predict the risks of explosive blast damage to build infrastructure. Cizelj et al. [3] likewise, presented a vulnerability assessment of blast-loaded structures. Shi et al. [4] also offered a method to assess progressive collapse in RC frame structures under blast loadings. Cullis et al. [5] ventured into evaluating the effects of different explosions and blast loads on buildings. Similarly, Fu [6] advanced a new method to estimate a tall building's response to blast loadings. He finally offered a comparison between his proposed method and alternative path method (APM). By the same token, Parisi and Augenti [7] assessed the performance of seismic resistant RC frame structures designed according to Eurocode 8, under blast loadings. They developed the intended blast scenarios in accordance with structural site quality and the amount of explosives required. Then, to evaluate the robustness of the building, they performed a pushdown analysis.

Asprone et al. [8] developed a probabilistic model for evaluating multi-hazard risk in buildings subject to blast threats in seismic-prone areas. This was achieved by simulating terroristic attack scenarios. The blast and seismic fragilities of the intended building were also calculated which yielded an evaluation of the collapse risk.

In the literature reviewed, it can be observed that all the scenarios developed to assess the robustness of a building

Article history: Received Jan 4, 2017; Accepted Mar 10, 2017

against blast loadings; the structure is only exposed to a blast load, or if it is simultaneously struck by a second load, such as seismic oscillations, then the structure is assumed to have the chance for recuperation and reparation. This means that, in these studies, calamitous events (e.g., earthquakes, explosions, fire, etc.) were assumed incompatible. In these cases, calamitous events are not considered simultaneous so their occurrence is not assumed to be in short intervals. Moreover, in all these studies calamitous events are supposed to be independent from one another; that is the occurrence of one event cannot possibly or conditionally cause the occurrence of a second event. In such situations, scenarios are developed based on blast uncertain parameters. Uncertain parameters include the explosive type used, its quantity and its distance from the target. In this study, we intend to consider seismic load along with blast loads, and as a result, these two events are considered compatible (they can occur simultaneously) and codependent (blast occurs if earthquake occurs). In such a way that during or immediately after an earthquake, a blast occurs due to the failure of thermal/mechanical installations and consequent gas leak in the building, without any chance for recuperation or reparation of the structure. Finally, it is manifested that under the proposed condition, the time of the blast would influence the uncertainty of the blast load.

On the other side, one can observe that in most strong or medium earthquakes along with critical earthquake load, gas explosive can increase the damages subjected to a structure due to mechanical and thermal failure of the installation. This factor highlights the significance of performing the current study so that one can evaluate the collapse rate of the structure with an appropriate method under such condition and also obtain an acceptable and correct assessment of structures subjected to these two critical loads.

2 Assessment methodology

If we consider an earthquake as a calamitous event in a building, the annual probability of structural collapse can be deduced from the following [9–11]:

$$P[\text{Collapse}]_{\text{EQ}} = P[\text{Collapse}|\text{EQ}] \times P[\text{EQ}], \quad (1)$$

where $P[\text{Collapse}]_{\text{EQ}}$ is the annual probability of collapse limit state of the building when the structure is exposed to an earthquake. $P[\text{Collapse}|\text{EQ}]$ is seismic fragility curve and $P[\text{EQ}]$ is the annual rate of seismic activities in the structural site. In other conditions, if a blast is considered a calamitous event in the building, the annual probability of collapse limit state of the building exposed to a blast ($P[\text{Collapse}]_{\text{Blast}}$) will be:

$$P[\text{Collapse}]_{\text{Blast}} = P[\text{Collapse}|\text{Blast}] \times P[\text{Blast}], \quad (2)$$

where $P[\text{Collapse}|\text{Blast}]$ is blast fragility; and $P[\text{Blast}]$ is the annual rate of blast in the intended structural site. On the other hand, if both earthquake and blast are considered calamitous events in a building, which are incompatible (that is: $P[\text{EQ} \cup \text{Blast}] = P[\text{EQ}] + P[\text{Blast}]$) and without any conditional relationship (that is: $P[\text{Blast}|\text{EQ}] = 0$), and the building is assumed to have enough time for recuperation and reparation after the earthquake, the annual probability of structural collapse under both seismic and blast loads ($P[\text{Collapse}]_i$) can be calculated in this way:

$$P[\text{Collapse}]_i = P[\text{Collapse}]_{\text{EQ}} + P[\text{Collapse}]_{\text{Blast}}. \quad (3)$$

It is necessary to remember that Eq. (3) has been used by Asprone et al. [8] as a model for tow-hazard risk assessment of structures.

In this paper, it is suggested that a blast occurs when an earthquake shakes a building, so that:

$$P[\text{Blast}|\text{EQ}] = \frac{P[\text{Blast} \cap \text{EQ}]}{P[\text{EQ}]}, \quad (4)$$

where $P[\text{Blast}|\text{EQ}]$ is the blast risk when an earthquake occurs; $P[\text{Blast} \cap \text{EQ}]$ is the simultaneous risk of blast and earthquake. Under these conditions, it is possible to determine the annual probability of structural collapse as a result of both earthquake and blast ($P[\text{Collapse}]_{\text{c}}$) as follows:

$$P[\text{Collapse}]_{\text{c}} = P[\text{Collapse}|(\text{Blast} \cap \text{EQ})] \times P[\text{Blast}|\text{EQ}] \times P[\text{EQ}]. \quad (5)$$

In Eq. (5), $P[\text{Collapse}|(\text{Blast} \cap \text{EQ})]$ is fragility due to seismic and blast load simultaneously. The purpose of the current research is calculation of $P[\text{Collapse}]_{\text{c}}$. Consequently, it is necessary to develop the fragility curve $P[\text{Collapse}|(\text{Blast} \cap \text{EQ})]$. To judge this curve, the necessary analysis is presented in two steps and then by developing scenarios, and taking into account uncertainties inherent in this study, occurrence or non-occurrence of progressive collapse is evaluated in each scenario. In the end, the fragility curve is analyzed. $P[\text{EQ}]$ is an engineering parameter and it is possible to measure this parameter with the use of Probabilistic Seismic Hazard Analysis (PSHA) in a site. $P[\text{Blast}|\text{EQ}]$, however, is not an engineering parameter. Yet, it is possible to decide on a rate by taking into account the history of earthquakes in the site which were followed by blasts.

3 Principal steps towards analysis

3.1 The first step of analysis

3.1.1 Local dynamic analysis of the blast

It is necessary that in each scenario a local dynamic analysis of the gas blast is carried out. There have been

studies on getting the chronology of blast pressure and modeling along with its application in the structure.

3.1.1.1 Gas explosion in confined spaces

Gaseous fuels burn in two different ways in the air. One type of burning is the usual fire in which fuel integrate with oxygen immediately before burning. In the other form, oxygen and fuel blend together without any ignition. Any spark in this situation will cause a huge burning in a glance which is called explosion. It is because of higher burning rate. Explosion is actually extreme and sudden release of energy. The power of energy during explosion depends on diffusion velocity of released energy [12,13]. Explosion can be classified to three categories regarding to the place in which the explosion occurs: Confined Explosion, Semi-Confined Explosion and Unconfined Explosion. Confined Explosions happen in closed places such as tanks, vessels, closed rooms and underground utilities [14]. Many factors affect confined explosion, such as shape and size of the environment, fuel type, fuel to air ratio, initial pressure, initial temperature, initial turbulence, ignition source [15,16].

3.1.1.2 Methods for modeling gas explosion and selecting an appropriate method

Many researches have been conducted for gas explosion modeling. Generally, modeling of gas explosion can be categorized in four classes: Empirical Models, Phenomenological Models, Computational Fluid Dynamic (CFD) Models, and Advanced CFD Models. Recently, a study was conducted on all above-mentioned models, which explains strengths and weaknesses of each models and also all their subsets [17,18].

As mentioned above, pressure behavior could be simulated through CFD techniques. However, the CFD simulation needs a lot of time, cost and detailed information about the explosion conditions. Therefore, the CFD simulation is not suitable for practical safety management, and analytical approaches are considered to be useful [19]. In the analytical approaches, the following differential equation derived by theoretical analysis is used to estimate the pressure behavior in the confined spherical vessel [20−22]:

$$S=\frac{R}{3(P_{\mathrm{e}}-P_0)}\left(\frac{P_0}{P}\right)^{1/\gamma}\left[1-\left(\frac{P_0}{P}\right)^{1/\gamma}\frac{P_{\mathrm{e}}-P}{P_{\mathrm{e}}-P_0}\right]^{-2/3}\frac{\mathrm{d}P}{\mathrm{d}t}, \tag{6}$$

where S is the burning velocity, R the vessel radius, γ the ratio of specific heats, t the time, and P the pressure in the vessel. Subscript "0" indicates the initial condition, and "e" the condition when the explosion is completed. Numerical integration of Eq. (6) provides the pressure development as a function of the time from the ignition. In this study is used from Eq. (6) to investigate the pressure behavior in the gas vessels when the gas explosion is happened in each scenario.

3.1.2 Non-linear dynamic time history analysis (NLTHA)

A complex but a more accurate method to evaluate inelastic demand of structure is using accelerogram [23−25]. In this study, NLTHA was used to assess the seismic damage scale.

3.2 The second step towards an analysis: general pushdown analysis

For a structure subject to gravitational loads, collapse mechanism should be assessed by employing a general analytic method. To this aim, a 3-D model of the building is required, because a two-dimensional analysis would produce a bigger quantity for the structure's load bearing capacity against abnormal loadings [26,27]. Push-down analysis is widely recognized as a valuable method to evaluate the load bearing capacity of structures [28]. Push-down analysis is a non-linear (static or dynamic) analysis in which the damaged structure subject to gravitational loadings, which accumulate due to movements in the control point, is analyzed up to the moment of collapse or to the point when numerical convergence rate decreases. Control point is often assumed to exist in a member which has lost its bearing capacity (like columns). Collapse, accompanied by a decisive plastic hinge rotation or brittle fractures, causes a member to detach from the structural system. Push-down analysis includes $P-\Delta$ effects, yet equation for large displacements are not used, because based on the findings in other pieces of research; incremental resistance mechanism is assumed negligible [29−31].

4 Evaluating progressive collapse and presenting fragility curve

In this study, regarding blast loading uncertain parameters, some scenarios were developed. Geometric location of the blast on the ground plan and the blast time are from among uncertain parameters. So atmospheric dispersion modeling was employed to produce the scenario of the blast condition. By meshing the plan and selecting critical points in each surface element, the blast condition on the plan surface was finally obtained. It was assumed that the blast occurred due to installation failure and consequent gas leak. So the explosive substance is the Compressed Natural Gas (CNG) confined in the gas pipes. As a result, parameters of explosive material and quantity are certain. To determine the latitude of surface elements, a blast

scenario in the minimum distance to the target point was considered and changes in the maximum stress on the surface were studied and the width and length of the elements were measured. Blast time is considered to be a part of the duration of intense oscillations or a bit after that. So each scenario is introduced with a geometric location and a determinate time of blast. According to the general services administrations (GSA) code [32], two parameters (demand/capacity ratio and maximum allowable local collapse area) are introduced.

4.1 Demand/capacity ratio (DCR)

According to the GSA code (2003), The Demand/Capacity Ratio (DCR) will be:

$$\mathrm{DCR} = \frac{Q_{\mathrm{UD}}}{Q_{\mathrm{EC}}}, \tag{7}$$

where Q_{UD} is the active force (demand); and Q_{EC} is the expected capacity which can be flexural, shear or axial force. But to calculate DCR these two parameters should be of the same quality. DCR can be regarded as a failure criterion in a structural element. In a way that if an element has an unallowable DCR it would be eliminated from the structural system. Permissible DCR limit for a normal building structure is less than 2 and for an exceptional building structure it is less than 1.5. According to UFC 4-023-03 [33] code, LS (Life Safety, see Ref. [34]) is the criterion to accept a column for non-linear dynamic analysis. So if the plastic hinges on the two sides of the column exceed the criterion, the member is useless and will break (the element has an unallowable DCR).

4.2 Maximum allowable local collapse area

If a vertical member (a column) in a structural system has an unallowable DCR it should be eliminated. By removing the column, a maximum allowable local collapse area is created in its vicinity (Fig. 1).

The first step towards an analysis of the phenomenon is to study both the blast and the earthquake based on aforementioned uncertainties and with taking into account diverse conditions in each scenario. Then, DCR should be measured for each column. If DCR of a column is not in the allowable area, it should be eliminated and maximum allowable local collapse area should be estimated for that removed column. This process would be repeated for all scenarios and in the second step a push-down analysis of the damaged structure would be carried out. If after the second step is taken, a column with an unallowable DCR is detected which is not within the allowable local collapse area measured in the first step, it means that in this scenario, collapse would no longer be local, but has a great potential to be progressive.

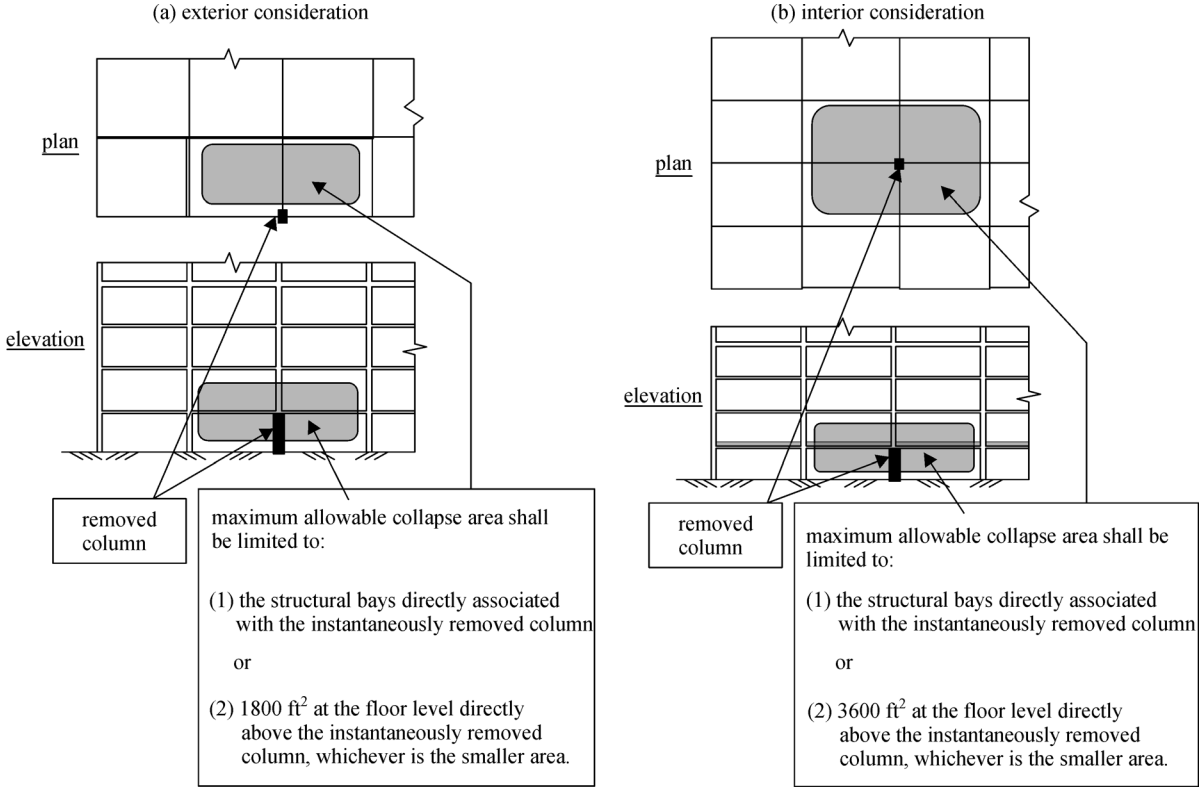

Fig. 1 Maximum allowable local collapse area in a structure where a column is removed. (a) External column removed; (b) internal column removed [32]

Progressive collapse in each scenario can be described with Bernoulli distribution function. In this method, when progressive collapse happens in a scenario, I_C (It is an index), would be 1, and if progressive collapse does not happen, I_C would be 0. Finally, if the N_{Sim} has been considered as the number of all scenarios used, then fragility curve can be developed as:

$$P[\text{Collapse}|(\text{Blast} \cap \text{EQ})] = \frac{\sum_{i=1}^{N_{Sim}} I_C}{N_{Sim}}. \quad (8)$$

5 Numerical example

5.1 Explaining structural model

The building studied is a public five-story high RC building designed based on Eurocode 8 [35]. Figures 2 and 3 show the 3-D structure and the ground plan, respectively. Column dimensions on the first and second floor are 0.30 × 0.60 m^2. On other floors column dimensions vary and are 0.30 × 0.50 m^2. Two types of beams are also used, A and B, which are 0.30 × 0.50 m^2 and 0.30 × 0.80 m^2, respectively. Column height on all floors is 3 m, but on the fourth floor it is assumed 4 m. Gravity load includes dead and live load. Dead load value for floors is 550 kg/m^2, the live load is 200 kg/m^2, and finally, the value of the roof floor has been considered to be 150 kg/m^2. Other types of loading such as wind load and snow load and also soil-structure interaction have not been considered. Compressive strength of the concrete and the thickness of concrete slab in the floors were considered 250 kg/m^2 and 25 cm.

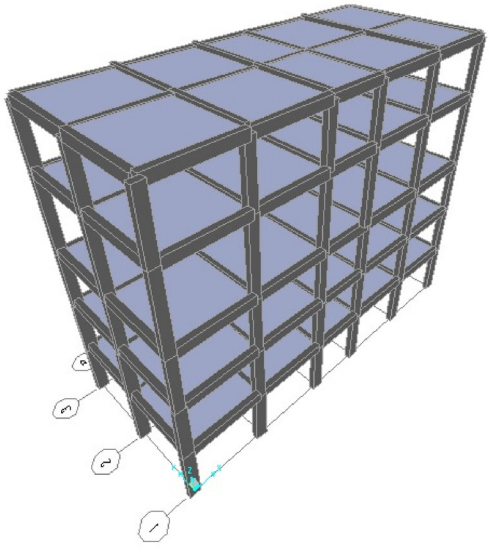

Fig. 2 A three dimensional model

5.2 Blast uncertain parameters

As was discussed earlier, scenarios are developed based on blast uncertain parameters. It is assumed that mechanical installations are on the first floor, so the blast occurs on the plan of the first floor. In order to assess the geometric location of the blast (index points in each surface element) in an atmospheric dispersion modeling, a blast load scenario with peak pressure and minimum time and distance from the target point (the center of the first floor plan) is enacted. In this situation, changes in the maximum surface stress which take place as an effect of the blast pressure wave on the plan of the first floor (Fig. 4) will be analyzed.

It is clear that a change in the maximum surface stress is about 1.9 m in length and 4 m in width. Considering the present situation, the first floor plan is meshed and index points (the center of each surface element) is assessed (Fig. 5). Doing this, twenty different blast conditions (index points) were created and in each condition a blast scenario took place.

Another blast uncertain parameter is blast time. In this study, four different blast times are considered. For the first three models, the blast occurs during intensive seismic oscillations. To this aim, the duration of these intensive oscillations is evaluated based on a specific accelerogram. This time period is divided into three sections. In the center of each section, a blast occurs simultaneously with an earthquake. In the fourth scenario, the period of intensive oscillations has ceased. That means, a short time after the earthquake, a blast occurs. Regarding the uncertain parameters mentioned earlier, for each accelerogram, eighty scenarios (twenty blast conditions each studied in four different blast time) would be created.

5.3 Evaluation of net explosive quantity (NEQ)

The explosive material is Compressed Natural Gas (CNG). Seismic sensor installed in gas contours to detect earthquakes and shut off of the gas flow during an earthquake increases security while decreasing the damages caused by gas explosive during occurrence of an earthquake. The system of the building under study has a seismic sensor in the gas contour. Therefore, the sensor will act during an earthquake and it will shut off the gas flow in the contour. The volume of the gas trapped in the gas pipes from gas contour to the mechanical installations during an earthquake with gas pipes broken is considered as NEQ. In such condition, NEQ has certainty and can be calculated. For this purpose, first of all and according to diameter and length of the pipeline, we should calculate the volume of the CNG trapped from gas contour to mechanical installations. Finally, considering CNG density (0.65 kg/m^3), one can obtain the NEQ.

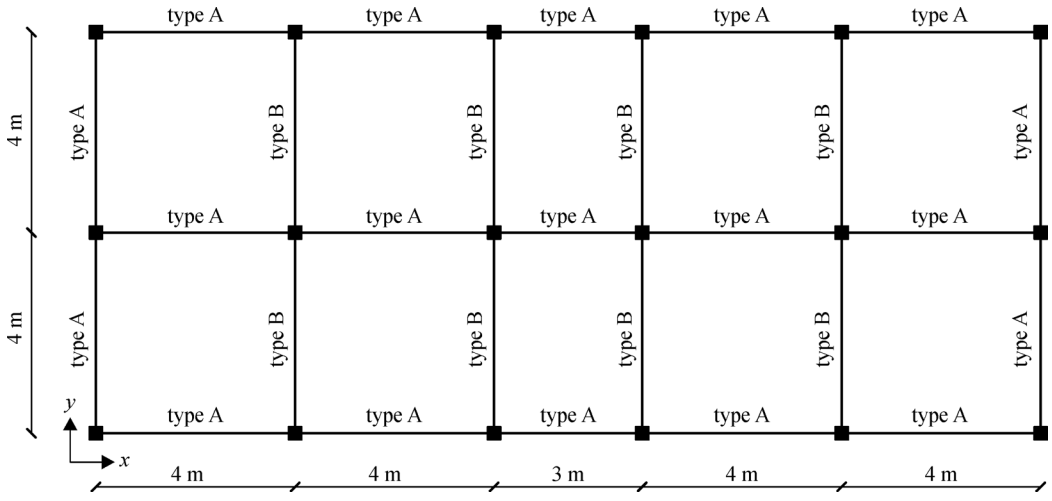

Fig. 3 Ground floor plan

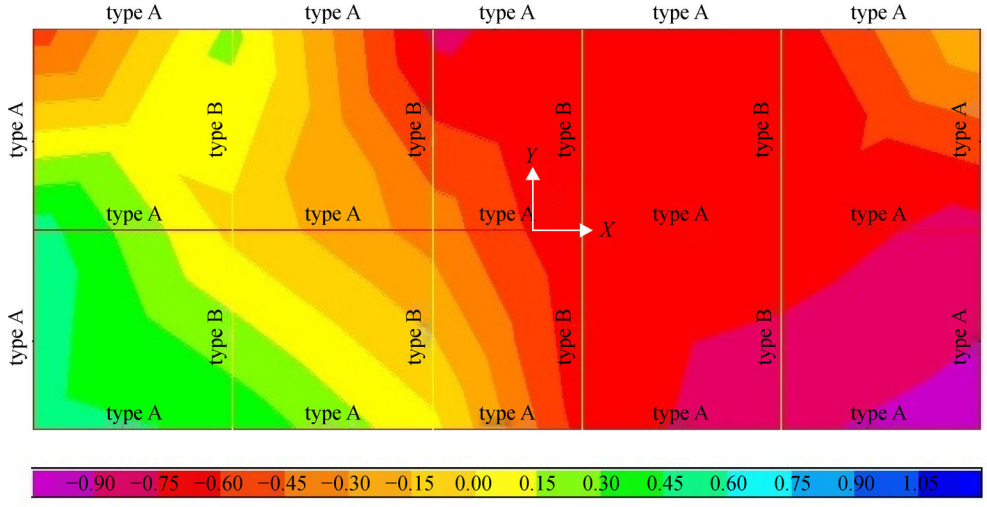

Fig. 4 Maximum surface stress exerted on the plan of the first floor due to blast pressure wave

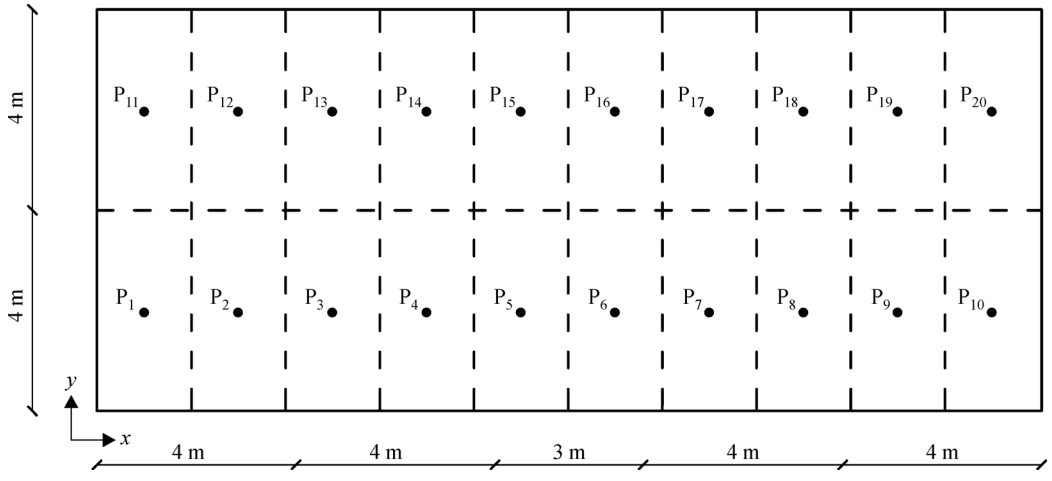

Fig. 5 Meshing the plan of the first floor and the location of index points in each structure element

5.4 Uncertainties in selecting earthquake records

In this piece of research, seven ordinary earthquake records have been used. These records are obtained from PEER institute database [36]. The magnitude of the earthquakes chosen for study ranges from 6.5 to 7.5 and the distance from the epicenter to the construction site is between 15 and 30 km. Grade C and D soil types with 5 percent liquefaction also exist. These records have been converted and then Scaled with SeismoSignal software [37]. According to what Trifunac and Brady [38] achieved in their study, if the total energy entering the building during the earthquake is IE (Input Energy), then the beginning of the seismic activity is when total energy reaches 5% of the IE and its end is when the total energy hits 95% of the IE. Intensive oscillation period is then, the time period between the initiation phase and termination point. For each earthquake record selected for this study the period of strong earthquake ground motion is calculated in Seismo-Signal software. Table 1 presents the earthquake records selected for this study.

Since 80 scenarios were defined for each seismic record, we would have 560 scenarios for the 7 accelerograms used. Figure 6 illustrates the process of developing scenarios for each earthquake record.

5.5 Push-down analysis

In this study, push-down analysis is a non-linear static analysis. According to UFC 2009 code [33], push-down analysis would follow this procedure:

(a) Increased gravity loads for floor areas above removed column (G_N):

$$G_N = \Omega_N[1.2DL + (0.5LL \text{ or } 0.25SL)], \tag{9}$$

where G_N is incremental gravitational force for non-linear static analysis; *DL*, *LL* and *SL* are dead load, live load and snow load (which snow load is not considered in this study), respectively; and Ω_N is Dynamic Increase Factors (DIF). In GSA code [32], for dead and live loads, DIF equals 2. Ruth and et al. [39] studied the effect of DIF reduction on non-plastic systems by analyzing steel moment frame buildings. For RC frame buildings, DIF ranges from 1.5 as the upper bound to 1−1.4 as lower bound. In the research carried out by Tsai and Lin [29], it was shown that DIF for RC moment frame buildings can be reduced from 2 to 1.2. Yet, UFC code [33] has offered a new method for determining suitable DIF measures based on allowable deformation and performance level:

$$\Omega_N = 1.04 + \frac{0.45}{\theta_{ls}/\theta_y + 0.48}, \tag{10}$$

where θ_{ls}/θ_y is the smallest ratio of plastic rotation of structural element to yield rotation.

(b) Gravity loads for floor areas away from removed column (G):

$$G = 1.2DL + (0.5LL \text{ or } 0.25SL). \tag{11}$$

In keeping with previous discussions, after the first analytical step in each scenario and removal of columns with unallowable DCR, the second step is taken. Since a column is removed in the first phase, it is possible to practice loading model (a) or (b) in the second step of analysis. Figure 7 demonstrates how loading in this phase occurs.

5.6 Progressive collapse and fragility curve

The first and second steps of analysis were performed for all the 560 scenarios. Sap2000 software, version 18 [40], was used for analysis. As mentioned, the first step of analysis relates to the simultaneous effect of earthquake load and the pressure resulted from the blast experienced by the structure. It has been applied on the structure through defining the functions of time history of the selected records and their nonlinear time history dynamic analysis and a definition of pressure wave resulted from explosion and its dynamic-based analysis in the software. In this stage, the time of starting the dynamic analysis resulted from explosion during the time history dynamic

Table 1 Selected seismic records

No.	EQ. name	station	peak ground acceleration (PGA) (g)	peak ground velocity (PGV) (cm/s)	peak ground displacemen (PGD) (cm)	start time[1] (s)	end time[2] (s)	difference (s)[3]
A_1	Kocaeli, Turkey	Atakoy	0.164	16.2	11.59	11.74	24.19	12.45
A_2	Northridge	Beverly Hills	0.617	4.8	8.57	0.50	2.01	1.51
A_3	Tabas	Boshrooyeh	0.107	13.7	10.50	1.04	3.08	2.04
A_4	Loma Prieta	Halls Valley	0.134	15.4	3.30	2.41	8.88	6.47
A_5	Landers	Morongo Valley	0.188	16.6	9.45	3.51	15.89	12.38
A_6	Cape Mendocino	Rio Dell Overpass	0.385	43.9	22.03	0.43	1.44	1.01
A_7	Imperial Valley	Chihuahua	0.270	24.9	9.08	0.65	5.07	4.42

[1] Initiation phase of strong earthquake ground motion
[2] Termination phase of strong earthquake ground motion
[3] Duration of strong earthquake ground motion

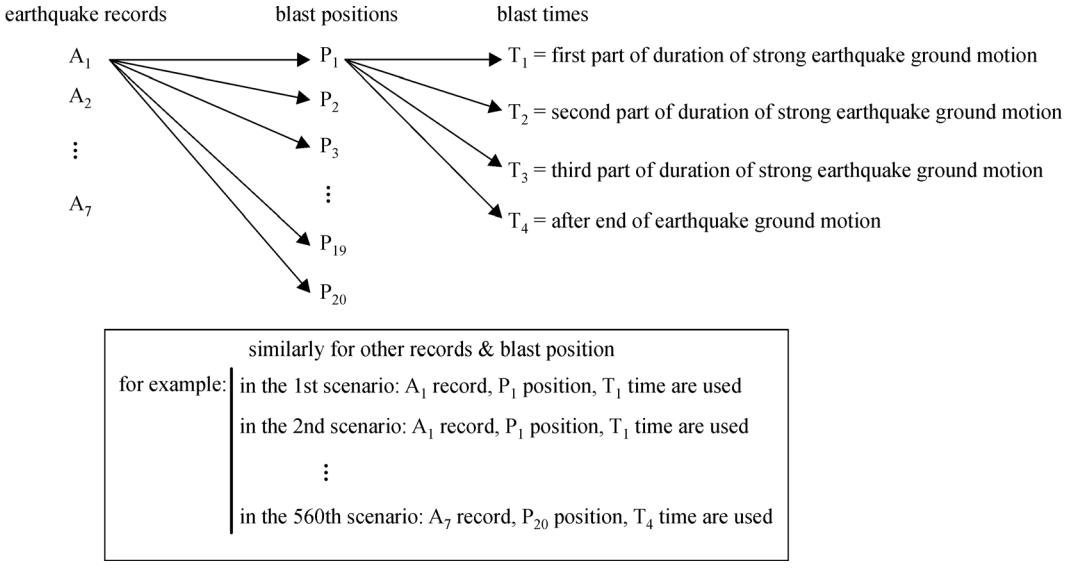

Fig. 6 Developing scenarios

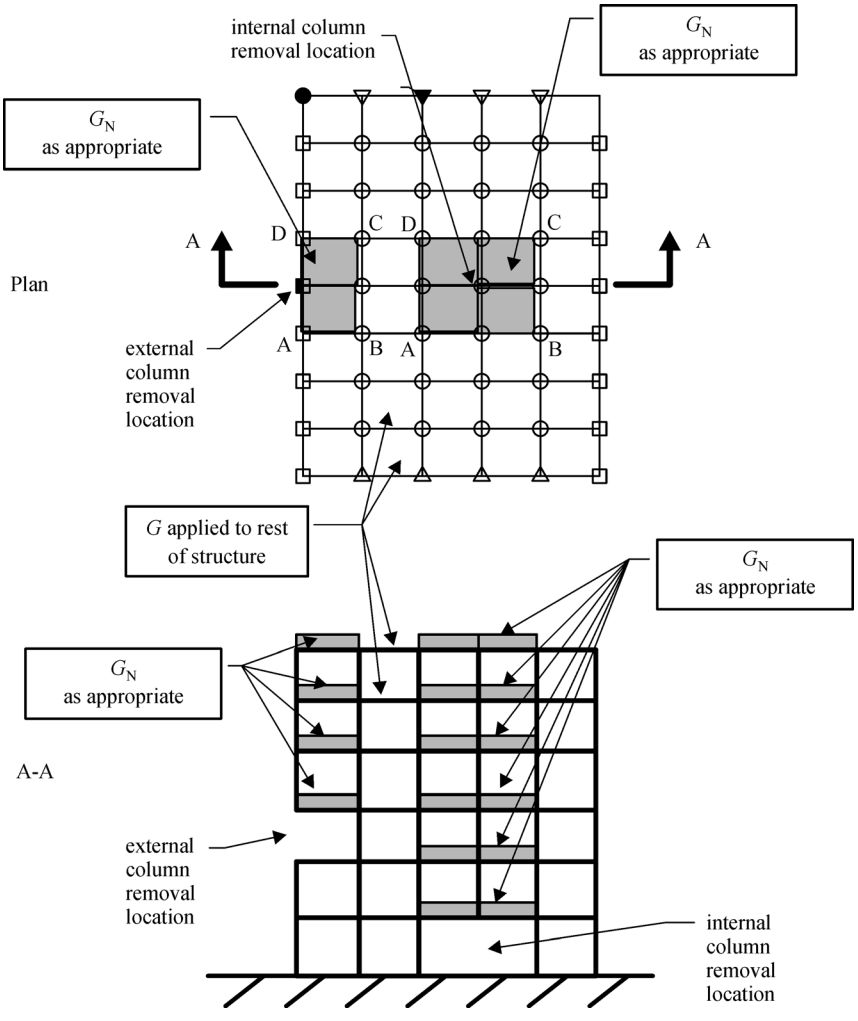

Fig. 7 The way G_N or G is loaded on the structure [32]

analysis of the earthquake in each scenario is of great significance. In the second step of the analysis, one nonlinear static analysis resulted from times of gravity with dynamic Increase factor has been applied.

Figure 8 presents the total deformity of the structure in scenario 13 under the P_4 blast condition, T_1 blast time and A_1 record. In this scenario, it was observed that progressive collapse and soft-story mechanism [41,42] set in. Soft-story mechanism is the formation of plastic hinges on the two sides of the columns, which occurs on the fourth floor of the intended building, and is regarded as a collapse mechanism. Likewise, maximum DCR value and the occurrence of progressive collapse rate in all scenarios were calculated.

All in all, for each blast condition, 28 scenarios (changes in blast time and seismic records) and for each blast time 140 scenarios (changes in blast conditions and seismic records) and for each seismic record 80 scenarios (changes in blast conditions and blast time) were developed. Figure 9 illustrates how many progressive collapses existed for each uncertain parameter.

Figure 9(a) shows that locations closer to the target point (the center of the first floor plan) (that is P_4, P_5, P_6, P_7, P_{14}, P_{15}, P_{16}, P_{17}) exhibit the most intense progressive collapse in their relevant scenarios. So it can conclude that these points are critical conditions. Similarly, Fig. 9(b) proves the same point, showing that when the blast occurred simultaneously with the earthquake (T_1, T_2, T_3) progressive collapse was more prevalent than in conditions when the blast only followed the earthquake. From among different time parameters, T_2 relevant scenarios (where it is predicted that PGA (Peak Ground Acceleration) existed in this range) progressive collapse was more intense. So T_2 can be regarded as critical time.

In the end, on the basis of cumulative distribution function (Eq. (8)), and progressive collapse probability due to critical DCR changes, fragility curve was developed (Fig. 10).

A DCR limit state of 2 can be assumed as a criterion for the failure or collapse of a structure [32]. So, regarding the fragility curve developed, when DCR equals 2, the collapse limit state of the structure would be 0.22. General consequences in a structure should correspond with its primary event. Robustness in a structure prevents a local

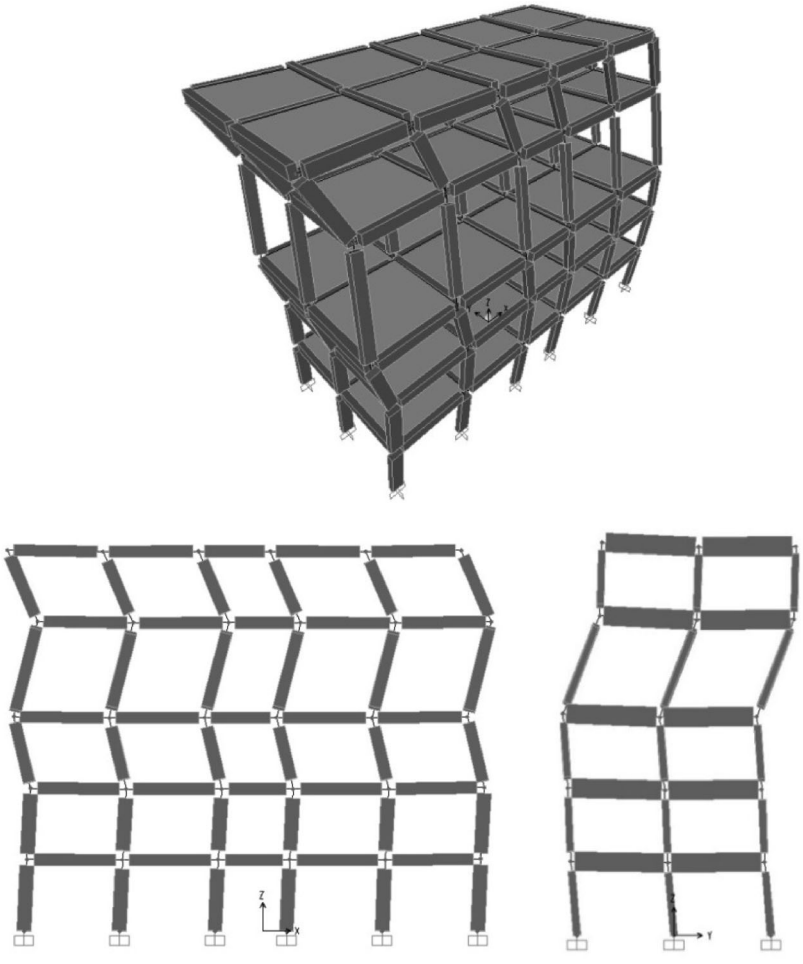

Fig. 8 Structural deformation in scenario 13

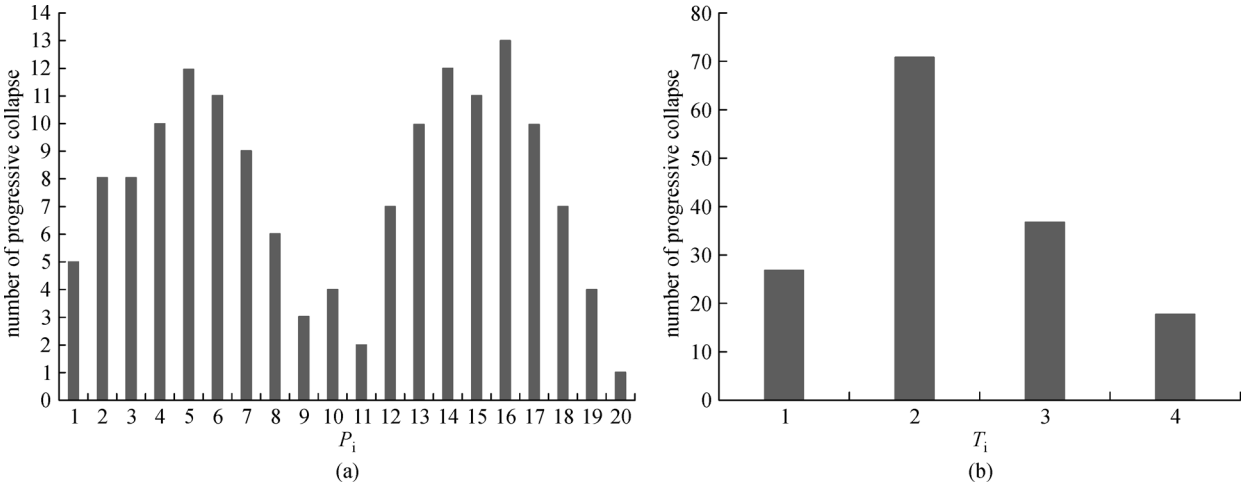

Fig. 9 The number of progressive collapses for each uncertain parameter. (a) Blast condition changes; (b) blast time changes

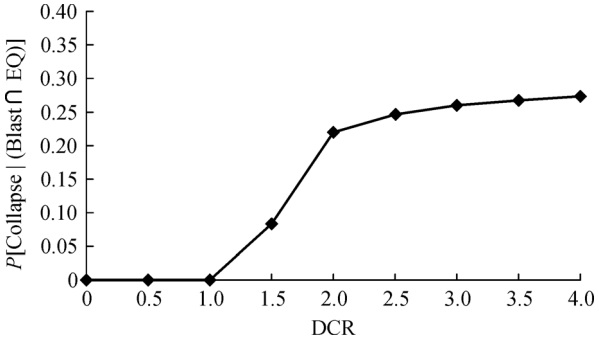

Fig. 10 Fragility curve of the intended structure

damage to be changed into a comprehensive damage [43,44]. Robustness depends, on one side, on inner properties of a structure such as redundancy, ductility, progressive collapse and key elements, and also on the type of scenarios in which one unpredicted critical event can lead to damage or collapse, on the other side [45,46]. The importance of robustness is known in most modern structural design codes; however, it has not been addressed in detail. There is one possibility of collapse in relation to risky robustness index. In this possibility, there is a basic relationship between robustness with reduced probability of P[Collapse|Blast ∩ EQ] [47–49].

According to the fragility amount obtained in the current study, one suitable robustness of the structure can be observed. One reason of the obtained result is utilization of modern structural design code (Eurocode 8) for this structure. Since in this regulation, the importance and place of the robustness of the structure has been recognized, in addition, in regulations relating to structure designing while considering the inner properties of the structure the suitable robustness will be obtained. In other words, it can be expected that the final damage and consequences of critical events in such structures correspond to the initial damages of these critical events.

5.7 Evaluation of annual rate of earthquake occurrence and the parameter of P[Blast|EQ]

Another parameter to determine the annual collapse risk of a structure is to predict the annual occurrence rate of earthquakes. According to Iranian code of practice for seismic resistant design of buildings [50], in 50 years of a structure's life, there is a 10 percent probability that an earthquake would occur. That is the return period is 475 years. So annual occurrence rate of earthquakes (P[EQ]) is about 0.0021.

P[Blast|EQ] is not engineering parameter and precise parameter. However, several factors are influential in probabilistic assessment of this parameter. In other words, it depends on improvements in the building industry and people's knowledge in using materials with high safety factor in thermal and mechanical installations, fabric, life and geometrical configuration of gas pipes in a building on one side, and on seismicity of the building construction site, on the other. It can be estimated by Poisson Theory. The Poisson Theory will be:

$$P(y) = \frac{(\lambda t)^y \mathrm{e}^{-\lambda t}}{y!}. \tag{12}$$

In the Equation (12), $P(y)$ is the probability of occurrence of the event, λ parameter is the occurrence rate of the event, y parameter is the number of occurrence of the event, t parameter is time period. One occurrence rate of explosion (as a λ) is equal to 5×10^{-3} [51]. So, probability of occurrence of one explosion in 50 years, which is practical lifetime of structure, ($t = 50$, $y = 1$), will be:

$$P(y) = \frac{(\lambda t)^y \mathrm{e}^{-\lambda t}}{y!} = \frac{(5 \times 10^{-3} \times 50)^1 \mathrm{e}^{(-5\times 10^{-3}\times 50)}}{1} \cong 0.20. \tag{13}$$

Therefore, the probability of occurrence of explosion can be assessed as 20 percent. Approximately and based on statistics [52], in the accident region, 65% of the different blast situations are the ones from gas leak as a result of earthquake. Hence the possibility of earthquake-related blast is 13% (that is: $65\% \times 0.20 = 13\%$).

6 Discussion on the case study

According to the assessment of influential factors in the annual probability of structural collapse, it can be concluded that:

$$P[\text{Collapse}]_c = 0.22 \times 0.13 \times 0.0021 = 6.006 \times 10^{-5}. \quad (14)$$

To compare the results obtained in this study with those of Asprone et al. [8], who had assumed earthquake and blast as two separate and independent events, and thus had presumed a recuperation chance to exist for the structures hit by earthquakes before a blast would occur, fragility in their studied structure was estimated to be 0.18 and collapse rate of structure was estimated to be 5.801×10^{-5}. Based on what is achieved in this study, fragility equals 0.22 and collapse rate amounts to 6.006×10^{-5}. The two parameters in this study have larger measurements than Asprone's. There are possibly two reasons for this difference: the first is that the two critical parameters were compatible and thus it was expected that they would result in a more intense damage. Second, the annual earthquake occurrence rate in Iran, based on Iranian code of practice for seismic resistant design of buildings is higher than Italy's National Institute of Geophysics and Volcanology, INGV's report of annual earthquake rate in this country [53]. As a result, the construction site in this study was more seismic prone.

7 Conclusions

In the present study, a method for evaluating the annual probability of collapse of a building structure was suggested. In this method, the concomitant (the events are compatible) effects of seismic and blast loads are studied, and blast occurrence is supposed to be dependent (a conditional relation exist between the two) on the occurrence of an earthquake. Atmospheric dispersion modeling was used to develop scenarios and non-linear dynamic time history analysis and local dynamic analysis due to blast load were also employed to produce an efficient analysis of progressive collapse in structures subject to gravitational loads.

This investigation provides a case study as well, producing an estimation of an RC moment frame structure's collapse rate:

Due to the inevitable existence of uncertain parameters, 560 scenarios were developed in atmospheric dispersion modeling. According to the estimations of critical DCR and progressive collapse rate in each scenario, the fragility of structure was calculated to be 0.22. In the vicinity of the target point, critical blast conditions and in the second phase of the duration of intensive oscillations, critical blast time was detected. Then the effects of these two events (earthquake and blast) as concomitant and simultaneous events were compared to the effect of these events as independent and incompatible. It was discovered that collapse rate and fragility were higher in the first instance.

Using modern structural design code (Eurocode-8) for the structure under study, since the importance and place of structure robustness has been recognized in this regulation, a suitable robustness is observed.

Moreover, it should be emphasized that the method proposed here is practiced on RC structures, yet it can also be applied to steel frames, masonry buildings, etc. for an evaluation of structural fragility.

References

1. Rong H C, Li B. Probabilistic response evaluation for RC flexural members subjected to blast loadings. Structural Safety, 2007, 29(2): 146–163
2. Stewart M G, Netherton M D. Security risks and probabilistic risk assessment of glazing subject to explosive blast loading. Reliability Engineering & System Safety, 2008, 93(4): 627–638
3. Cizelj L, Leskovar M, Čepin M, Mavko B. A method for rapid vulnerability assessment of structures loaded by outside blasts. Nuclear Engineering and Design, 2009, 239(9): 1641–1646
4. Shi Y, Li Z X, Hao H. A new method for progressive collapse analysis of RC frames under blast loading. Engineering Structures, 2010, 32(6): 1691–1703
5. Cullis I G, Schofield J, Whitby A. Assessment of blast loading effects—Types of explosion and loading effects. International Journal of Pressure Vessels and Piping, 2010, 87(9): 493–503
6. Fu F. Dynamic response and robustness of tall buildings under blast loading. Constructional Steel Research, 2013, 80: 299–307
7. Parisi F, Augenti N. Influence of seismic design criteria on blast resistance of RC framed buildings: A case study. Engineering Structures, 2012, 44: 78–93
8. Asprone D, Jalayer F, Prota A, Manfredi G. Proposal of a probabilistic model for multi-hazard risk assessment of structures in seismic zones subjected to blast for the limit state of collapse. Structural Safety, 2010, 32(1): 25–34
9. Ellingwood B R. Mitigating risk from abnormal loads and progressive collapse. Perform Construct Facil, 2006, 20(4): 315–323
10. Talebi H, Silani M, Rabczuk T. Concurrent multiscale modelling of three dimensional crack and dislocation propagation. Advances in Engineering Software, 2015, 80: 82–92
11. Talebi H, Silani M, Bordas S, Kerfriden P, Rabczuk T. A

computational library for multiscale modelling of material failure. Computational Mechanics, 2014, 53(5): 1047–1071
12. Talebi H, Silani M, Bordas S P A, Kerfriden P, Rabczuk T. Molecular dynamics/XFEM coupling by a three-dimensional extended bridging domain with applications to dynamic brittle fracture. International Journal for Multiscale Computational Engineering, 2013, 11(6): 527–541
13. Ghorashi S, Valizadeh N, Mohammadi S, Rabczuk T. T-spline based XIGA for fracture analysis of orthotropic media. Computers & Structures, 2015, 147: 138–146
14. Areias P M A, Rabczuk T, Camanho P P. Finite strain fracture of 2D problems with injected anisotropic softening elements. Theoretical and Applied Fracture Mechanics, 2014, 72: 50–63
15. Dobashi R, Kawamura S, Kuwana K, Nakayama Y. Consequence analysis of blast wave from accidental gas explosions. Proceedings of the Combustion Institute, 2011, 33(2): 2295–2301
16. Rabczuk T, Areias P M A, Belytschko T. A meshfree thin shell method for nonlinear dynamic fracture. International Journal for Numerical Methods in Engineering, 2007, 72(5): 524–548
17. Lea C J, Ledin H S. A Review of the State-of-the-Art in Gas Explosion Modelling. Harpur Hill, Buxton: Health and Safety Laboratory, Fire and Explosion Group, 2002
18. Areias P, Rabczuk T, Dias-da-Costa D. Element-wise fracture algorithm based on rotation of edges. Engineering Fracture Mechanics, 2013, 110: 113–137
19. Middha P, Hansen O R, Storvik I E. Validation of CFD-model for hydrogen dispersion. Journal of Loss Prevention in the Process Industries, 2009, 22(6): 1034–1038
20. Bradley D, Mitcheson A. Mathematical solutions for explosions in spherical vessels. Combustion and Flame, 1976, 26: 201–217
21. Dobashi R. Experimental study on gas explosion behavior in enclosure. Journal of Loss Prevention in the Process Industries, 1997, 10(2): 83–89
22. Zalosh R G. Explosion Protection, SFPE Handbook of Fire Protection Engineering, Chapter 3−16, 1995
23. Zhuang X, Zhu H, Augarde C. An improved meshless Shepard and least square method possessing the delta property and requiring no singular weight function. Computational Mechanics, 2014, 53(2): 343–357
24. Amiri F, Milan D, Shen Y, Rabczuk T, Arroyo M. Phase-field modeling of fracture in linear thin shells, Theoretical and Applied Fracture Mechanics, 2014, 69, 102–109
25. Alashker Y, Li H, El-Tawil S. Approximations in progressive collapse modeling. Structure Engineering, 2011, 137(9): 914–924
26. Areias P, Rabczuk T. Finite strain fracture of plates and shells with configurational forces and edge rotation. International Journal for Numerical Methods in Engineering, 2013, 94(12): 1099–1122
27. Amiri F, Anitescu C, Arroyo M, Bordas S, Rabczuk T. XLME interpolants, a seamless bridge between XFEM and enriched meshless methods. Computational Mechanics, 2014, 53(1): 45–57
28. Cai Y, Zhuang X, Zhu H. A generalized and efficient method for finite cover generation in the numerical manifold method. International Journal of Computational Methods, 2013, 10(5): 1350028
29. Tsai M H, Lin B H. Investigation of progressive collapse resistance and inelastic response for an earthquake-resistant RC building subjected to column failure. Engineering Structures, 2008, 30(12): 3619–3628
30. Rabczuk T, Zi G, Bordas S, Nguyen-Xuan H. A geometrically non-linear three-dimensional cohesive crack method for reinforced concrete structures. Engineering Fracture Mechanics, 2008, 75(16): 4740–4758
31. Zhuang X, Augarde C E, Mathisen K M. Fracture modeling using meshless methods and level sets in 3D: Framework and modeling. International Journal for Numerical Methods in Engineering, 2012, 92(11): 969–998
32. General Services Administration (GSA). Progressive collapse analysis and design guidelines for new federal office buildings and major modernization projects GSA. 2003
33. US Department of Defence. Design of buildings to resist progressive collapse, Unified Facilities Criteria, UFC 4-023-03. 2009
34. Federal Emergency Management Agency. Guidelines for seismic rehabilitation of buildings, FEMA 273, NEHRP. 1997
35. Comité Européen de Normalisation. Design of structures for earthquake resistance, Eurocode 8. 2005
36. Next Generation Attenuation (NGA). Project strong motion database. 2005
37. Seismosoft Company. Seismosignal earthquake engineering software solutions, Version 5.1.0. 2012
38. Trifunac M D, Brady A G. A study on duration of strong earthquake ground motio. Bulletin of the Seismological Society of America, 1975, 65: 581–626
39. Ruth P, Marchand K A, Williamson E B. Static equivalency in progressive collapse alternate path analysis: Reducing conservatism while retaining structural integrity. Perform Construct Facil, 2006, 20(4): 349–364
40. SAP. 2000. Structural analysis program. Version 18. California: Computers and Structures, Inc. 2015
41. Zhuang X, Huang R, Zhu H, Askes H, Mathisen K. A new and simple locking-free triangular thick plate element using independent shear degrees of freedom. Finite Elements in Analysis and Design, 2013, 75: 1–7
42. Zhuang X, Augarde C, Mathisen K. Fracture modelling using meshless methods and level sets in 3D: Framework and modelling. International Journal for Numerical Methods in Engineering, 2012, 92(11): 969–998
43. Abdollahzadeh G R, Faghihmaleki H. A method to evaluate the risk-based robustness index in blast-influenced structures. Earthquakes and Structures, 2017, 12(1): 47–54
44. Abdollahzadeh G R, Faghihmaleki H. Seismic-explosion risk-based robustness index of structures. International Journal of Damage Mechanics, 2016, doi: 10.1177/1056789516651919
45. Faghihmaleki H, Najafi E K, Aini A H. Seismic rehabilitation effect in a steel moment frame subjected to tow critical loads. International Journal of Structural Integrity, 2017, 8(1): 1–11
46. Abdollahzadeh G R, Faghihmaleki H. Effect of seismic improvement techniques on a structure in seismic-explosive probabilistic two-hazard risk. International Journal of Structural Engineering, 2016, 7(3): 314–331
47. Faghihmaleki H, Nejati F, Roshan A M, Motlagh Y B. An evaluation of multi-hazard risk subjected to blast and earthquake loads in RC moment frame with shear wall. Journal of Engineering Science and Technology, 2017, 12(3): 636–647

48. Khaloo A, Nozhati S, Masoomi H, Faghihmaleki H. Influence of earthquake record truncation on fragility curves of RC frames with different damage indices. Journal of Building Engineering, 2016, 7: 23–30
49. Abdollahzadeh G R, Faghihmaleki H, Esmaili H. Comparing hysteretic energy and inter-story drift in steel frames with V-shaped brace under near and far fault earthquakes. Alexandria Engineering Journal, 2016
50. Building and housing research center. Iranian code of practice for seismic resistant design of buildings, 4th revision, Standard No. 2800. 2013
51. Asprone D, Jalayer F, Prota A, Manfredi G. Probabilistic assessment of blast-induced progressive collapse in a seismic retrofitted RC structure. In: The 14th World Conference on Earthquake Engineering, Beijing, 2008
52. Statistical Institute of Pooyesh. The major damages in the building structures due to a strong earthquake. Report No. 93-411. 2012 (Persian)
53. Continuation of assistance to the DPC for the completion and management of the seismic hazard map provided by ordinance PCM 3274 and planning for future developments. Project INGV-DPC. S1. 2007